Translational Oncology
www.transonc.com

Volume 12 Number 8 August 2019 pp. 1079–1085 1079

Intratumor Heterogeneity in Interstitial Fluid Pressure in Cervical and Pancreatic Carcinoma Xenografts[1,2]

Lise Mari K. Hansem, Ruixia Huang, Catherine S. Wegner, Trude G. Simonsen, Jon-Vidar Gaustad, Anette Hauge and Einar K. Rofstad

Group of Radiation Biology and Tumor Physiology, Department of Radiation Biology, Institute for Cancer Research, Oslo University Hospital, Oslo, Norway

Abstract

Preclinical studies have suggested that interstitial fluid pressure (IFP) is uniformly elevated in the central region of tumors, whereas clinical studies have revealed that IFP may vary among different measurement sites in the tumor center. IFP measurements are technically difficult, and it has been claimed that the intratumor heterogeneity in IFP reported for human tumors is due to technical problems. The main purpose of this study was to determine conclusively whether IFP may be heterogeneously elevated in the central tumor region, and if so, to reveal possible mechanisms and possible consequences. Tumors of two xenograft models were included in the study: HL-16 cervical carcinoma and Panc-1 pancreatic carcinoma. IFP was measured with Millar SPC 320 catheters in two positions in each tumor and related to tumor histology or the metastatic status of the host mouse. Some tumors of both models showed significant intratumor heterogeneity in IFP, and this heterogeneity was associated with a compartmentalized histological appearance (i.e., the tissue was divided into compartments separated by thick connective tissue bands) in HL-16 tumors and with a dense collagen-I-rich extracellular matrix in Panc-1 tumors, suggesting that these connective tissue structures prevented efficient interstitial convection. Furthermore, some tumors of both models developed lymph node metastases, and of the two IFP values measured in each tumor, only the higher value was significantly higher in metastatic than in non-metastatic tumors, suggesting that metastatic propensity was determined by the tumor region having the highest IFP.

Translational Oncology (2019) 12, 1079–1085

Introduction

Interstitial hypertension [i.e., elevated interstitial fluid pressure (IFP)] is a characteristic feature of malignant solid tumors [1]. Most experimental and human tumors show IFP values of 5 to 40 mmHg, whereas the IFP of most normal tissues ranges from −3 to +3 mmHg [2]. Studies of experimental tumors have revealed that high IFP correlates with poor and heterogeneous uptake of chemotherapeutic agents [3,4], resistance to radiation therapy by hypoxia-dependent as well as hypoxia-independent mechanisms [5,6], and invasive growth and lymph node metastasis [7–9]. Clinical studies have shown that highly elevated IFP is associated with poor disease-free and overall survival rates in locally advanced cancer of the uterine cervix treated with radiation therapy or chemoradiotherapy [10–14].

Comprehensive studies of the mechanisms leading to interstitial hypertension in tumors have been carried out, and these studies have revealed that tumors develop elevated IFP because of impaired angiogenesis, resulting in high resistance to blood flow, low resistance to transcapillary fluid flow, and poor lymphatic drainage [2,4,15]. The microvascular hydrostatic pressure is the principal driving force for interstitial hypertension in tumors [16]. Fluid is forced from the

Address all correspondence to: Einar K. Rofstad, PhD, Department of Radiation Biology, Institute for Cancer Research, Oslo University Hospital, Box 4953 Nydalen, 0424 Oslo, Norway. E-mail: einar.k.rofstad@rr-research.no

[1] Funding: This work was supported by the Norwegian Cancer Society and the South-Eastern Norway Regional Health Authority.

[2] Conflict of Interest: The authors have no conflicts of interest.

Received 8 March 2019; Revised 9 May 2019; Accepted 13 May 2019

1936-5233/19
https://doi.org/10.1016/j.tranon.2019.05.012

microvasculature into the interstitium where it accumulates, distends the extracellular matrix, and causes an elevation of the IFP. Differences in IFP between tumors result primarily from differences in microvascular hydrostatic pressure caused by differences in resistance to blood perfusion (i.e., differences in vessel diameter, tortuosity, and branching) [15].

Intratumor heterogeneity in IFP has been measured in a few experimental tumors by using the micropipette technique. In these studies, a micropipette IFP probe was moved stepwise from the tumor surface into the tumor center, and the IFP was measured along the track [17]. The measurements showed that the IFP is uniformly elevated in the central region of tumors and drops steeply to normal tissue values at the tumor surface [7,17,18]. Therefore, in most experimental studies investigating possible consequences of elevated IFP in tumors, IFP is measured in a single location in the tumor center by using the wick-in-needle method, a method that is more robust than the micropipette method [2,15]. This strategy requires that the hydraulic conductivity in the tumor interstitium is sufficiently high to level out possible consequences of any intratumor heterogeneity in microvascular hydrostatic pressure [15].

However, some investigators have made multiple IFP measurements with the wick-in-needle technique in human tumors, and studies of melanoma [19], colorectal carcinoma [20], cervical carcinoma [21], and breast carcinoma [20] have suggested that IFP may vary from region to region within the same tumor. Unfortunately, data relating the intratumor variation of the IFP measurements to biological properties of the tumor tissue were not provided in any of these studies. Because IFP readings may be influenced significantly by multiple needle insertions, measurements of intratumor heterogeneity in IFP with the wick-in-needle method are technically challenging [22], and consequently, it is possible that technical problems may have contributed substantially to the heterogeneity in measured IFP values in human tumors [19–21].

The purpose of the study reported in this communication was to determine conclusively whether tumors may show significant heterogeneity in IFP in the central region, and moreover, to reveal whether any heterogeneity may have consequences for the assessment of microenvironment-induced tumor aggressiveness. The study was based on the hypothesis that heterogeneous IFP in the central tumor region, if present, is caused by structures that prevent efficient fluid flow in the interstitial space. Consequently, detailed comparative studies of IFP and tumor histology were carried out using experimental tumor models (HL-16 and Panc-1) known to show significant intertumor heterogeneity of the extracellular matrix. Furthermore, to search for associations between heterogeneity in IFP and tumor aggressiveness, IFP values of HL-16 and Panc-1 tumors were related to their propensity to develop lymph node metastases.

Materials and Methods

Tumor Models

Adult (8–12 weeks of age) female BALB/c *nu/nu* mice, bred at our research institute, were used as host animals for xenografted tumors. The mice were maintained under specific-pathogen free conditions and were given sterilized food and tap water *ad libitum*. The HL-16 cervical carcinoma and the Panc-1 pancreatic carcinoma were used as tumor models. The cervical carcinoma model was established in our laboratory [23,24], and late generation HL-16 tumors initiated from our frozen stock as described earlier were used in this study [25]. The pancreatic carcinoma model was purchased from the American Type Culture Collection, VA, USA, and Panc-1 tumors were initiated from cells cultured in RPMI-1640 (25 mmol/l HEPES and L-glutamine) medium supplemented with 13% bovine calf serum, 250 mg/l penicillin, and 50 mg/l streptomycin [26]. Approximately 5.0×10^5 HL-16 cells or ~2.5×10^6 Panc-1 cells suspended in 10–30 μl of Hanks' balanced salt solution were inoculated intramuscularly into the left hind leg. Tumor growth was recorded, and tumor volume (V) was calculated as $V = \pi/6 \times a \times b \times c$, where a, b, and c are three orthogonal tumor diameters measured with calipers. Tumors were included in experiments when having grown to volumes of ~1000 mm^3 (HL-16) or ~500 mm^3 (Panc-1). Tumors of this size did not impair the mobility of the mice. Moreover, intramuscular A-07 tumors were used in control experiments [27]. The animal experiments were approved by the Norwegian National Animal Research Authority and were conducted in accordance with the Interdisciplinary Principles and Guidelines for the use of Animals in Research, Marketing, and Education (New York Academy of Sciences, New York, NY, USA).

Interstitial Fluid Pressure

IFP was measured in two different positions in the central region of each tumor, avoiding any possible influence by the IFP gradient in the tumor periphery (Figure 1*A*). The measurements were conducted by using Millar SPC 320 catheters equipped with a 2F Mikro-Tip transducer (Millar Instruments, Houston, TX, USA). Each catheter was inserted once in each tumor using a hypodermic needle, and after the insertion, IFP was recorded for several minutes at a single location. Before the insertion, the catheters were calibrated by determining the relationship between measured pressures and pressures imposed by water columns. Before measurements, the mice were anesthetized with 0.63 mg/kg fentanyl citrate, 20 mg/kg fluanisone, and 10 mg/kg midazolam. The body core temperature of the mice, recorded with a rectal probe, was kept at 37 °C during IFP measurements by using an adjustable heating pad, thus ensuring normal physiological conditions.

Histology and Immunohistochemistry

The tumors were resected after IFP was measured and fixed in phosphate-buffered 4% paraformaldehyde immediately after the resection. Tissue sections for histological examinations were cut in a central tumor plane parallel to the mouse flank and stained with hematoxylin and eosin (HE) or immunostained for collagen-I. Immunohistochemistry was carried out as described elsewhere by using a peroxidase-based assay [28]. An anti-collagen-I rabbit polyclonal antibody (Abcam, Cambridge, UK) was used as primary antibody, diaminobenzidine was used as chromogen, and hematoxylin was used for counterstaining. Fraction of collagen-I-positive tissue was used as a measure of the density of the extracellular matrix, quantified as described elsewhere [29].

Lymph Node Metastasis

To search for associations between tumor IFP and lymph node metastasis, tumor IFP was measured in mice showing highly enlarged external lymph nodes and mice without enlarged external lymph nodes. The mice were euthanized immediately after the IFP measurement, and external as well as internal lymph nodes were resected and subjected to detailed histological examination to validate or invalidate the assumed

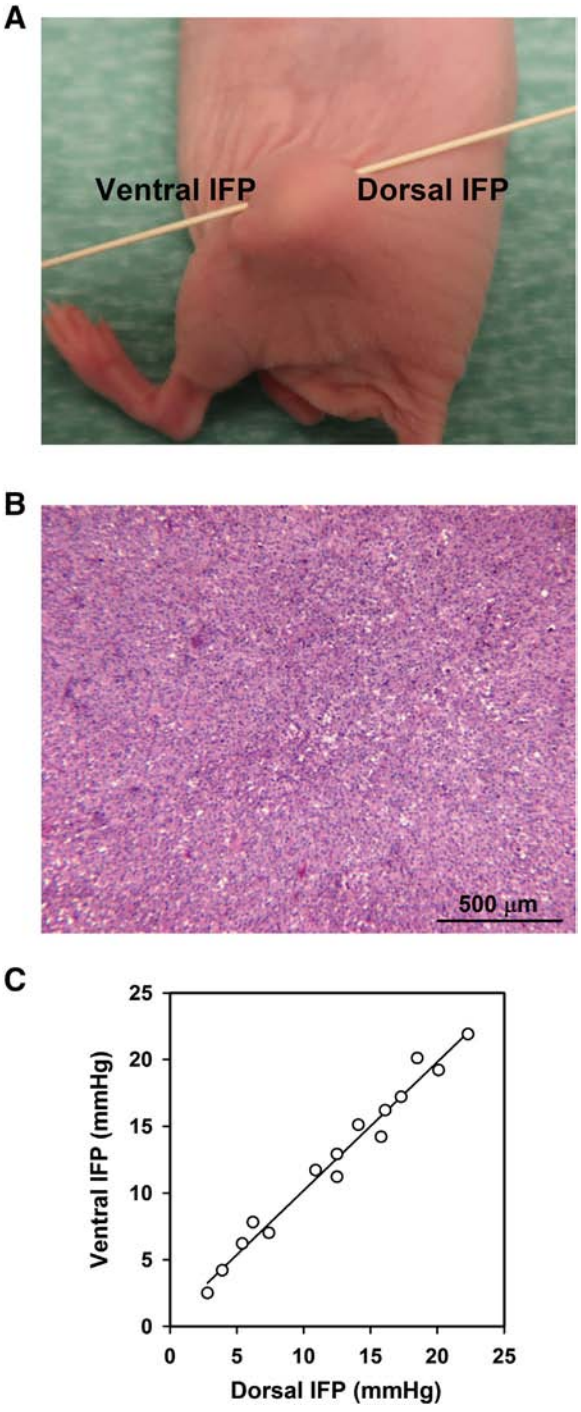

Figure 1. Measurement of tumor IFP. (A) IFP was measured centrally in the ventral and dorsal halves of intramuscular tumors. (B) Microphotograph showing that A-07 tumors have a homogeneous histological appearance. (C) IFP measured from the ventral side *versus* IFP measured from the dorsal side for A-07 tumors ($P < .0001$; $R^2 = .97$). Fifteen mice were included in the experiment. The points represent single tumors.

metastatic status. Six pairs of lymph nodes (i.e., the popliteal lymph nodes, inguinal lymph nodes, proper axillary lymph nodes, accessory axillary lymph nodes, medial iliac lymph nodes, and renal lymph nodes) were investigated as described elsewhere [30]. Examples of an enlarged lymph node with metastatic growth, a normal-sized lymph node without metastatic growth, and the histology of a lymph node with metastatic growth are presented in Figure 2.

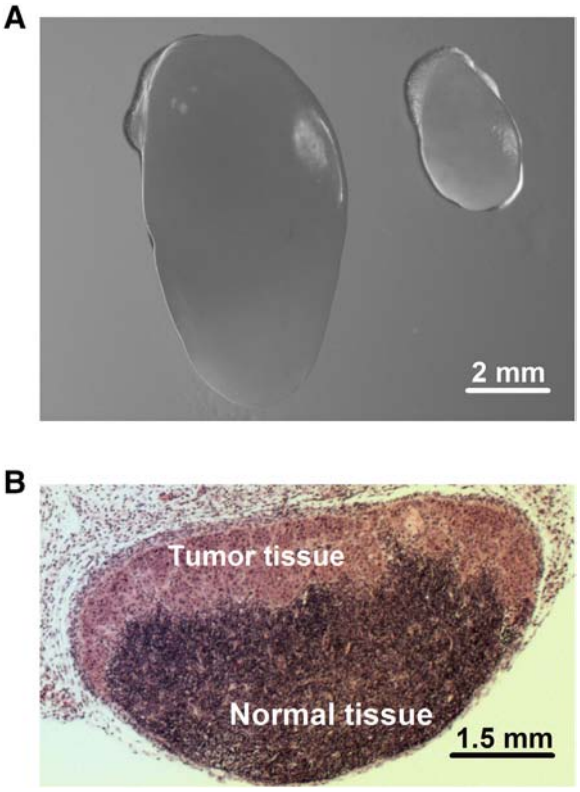

Figure 2. Lymph node metastasis. (A) Representative examples of an enlarged lymph node with metastatic growth and a normal-sized lymph node without metastatic growth. (B) Histological section prepared from a representative lymph node with metastatic growth.

Statistical Analysis

The Pearson product moment correlation test was used to search for correlations between parameters. Curve fitting was conducted by linear regression analysis. Comparisons of data were carried out by using the Student *t* test. The Kolmogorov–Smirnov method and the Levene method were used to verify normality and equal variance, respectively. Probability values of $P < .05$, determined from two-sided tests, were considered significant. The statistical analysis was conducted by using the SigmaStat statistical software.

Results

IFP was measured in two positions in each tumor, from the ventral and dorsal sides of the host mouse, as illustrated in Figure 1*A*. The IFP values recorded in these positions are expected to be equal in homogeneous tumors showing low resistance to interstitial fluid flow. To test this hypothesis, IFP measurements were carried out in A-07 tumors, which show a homogeneous histological appearance characterized by low cell density and a large extravascular extracellular volume fraction (Figure 1*B*). As expected, a strong one-to-one correlation was found between the IFP values measured in the ventral and dorsal halves of the tumors (Figure 1*C*).

Similar measurements in HL-16 tumors revealed that the IFP values recorded in the ventral and dorsal positions were nearly equal (i.e., IFP differed by less than 3 mmHg) in some tumors (Figure 3*A*) and highly different (i.e., IFP differed by more than 5 mmHg) in others (Figure 3*B*). Histological examination of HL-16 tumors showed that some tumors were homogeneous (Figure 3*C*), whereas others were divided into 2 to 6

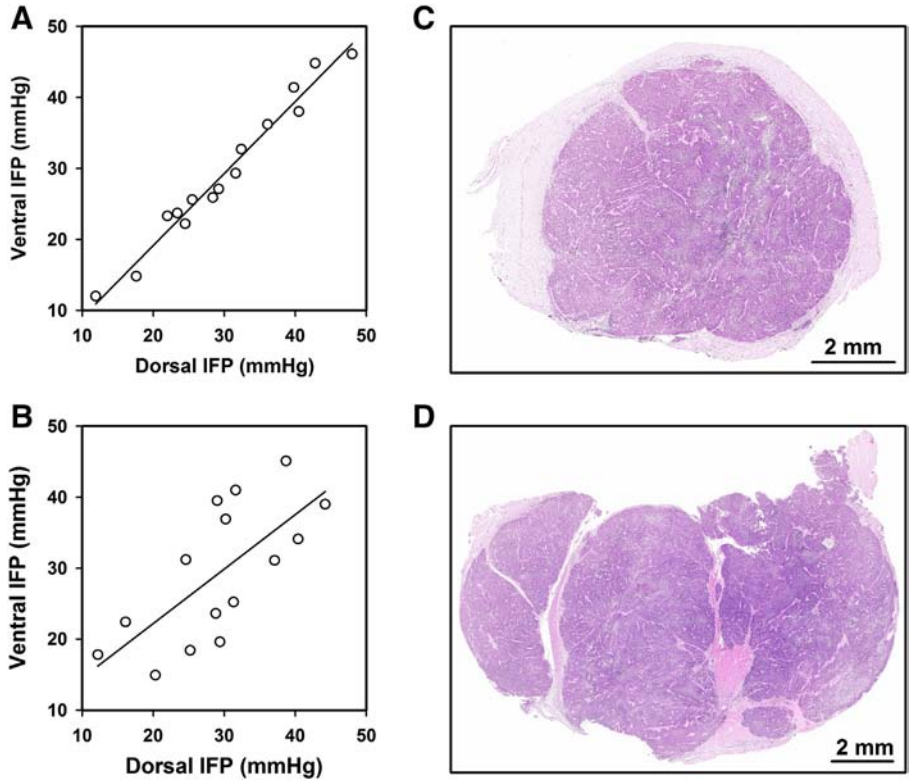

Figure 3. IFP in HL-16 tumors. IFP measured from the ventral side *versus* IFP measured from the dorsal side for (A) 15 tumors with a homogeneous histology ($P < .0001$; $R^2 = .97$) and (B) 15 tumors with a heterogeneous histology ($P = .0042$; $R^2 = .49$). The points represent single tumors. (C) Example of a tumor with homogeneous histology. (D) Example of a tumor with heterogeneous histology, showing that the tissue was divided into compartments by thick bands of connective tissue.

compartments separated by thick bands of connective tissue (Figure 3*D*). Comparative studies of IFP and histology revealed that the two IFP values were nearly equal in the tumors with a homogeneous histology, whereas the tumors with highly different IFP values showed a compartmentalized histological appearance.

The IFP values measured in the ventral and dorsal positions were nearly equal also in some Panc-1 tumors (Figure 4*A*), whereas other Panc-1 tumors showed highly different IFP values in these positions (Figure 4*B*). Examination of collagen-I-stained histological sections revealed that the density of the extracellular matrix differed substantially among individual Panc-1 tumors. In some tumors, the extracellular matrix occupied less than 30% of the tumor volume (Figure 4*C*), whereas more than 60% of the tissue stained positive for collagen-I in other tumors (Figure 4*D*). Measurements of IFP and collagen-I density in the same tumors revealed that the intratumor heterogeneity in IFP was associated with the density of the extracellular matrix. The two IFP values were nearly equal in the tumors with a collagen-I-positive fraction <30%, and the tumors showing two highly different IFP values had a collagen-I-positive fraction >60%.

To search for associations between IFP and lymph node metastasis, tumor IFP was measured in 10 mice with and 10 mice without highly enlarged external lymph nodes (i.e., with or without macroscopic metastases) of each tumor model. Histological examinations revealed that one of the HL-16 tumor-bearing mice and two of the Panc-1 tumor-bearing mice without macroscopic external metastases had developed microscopic lymph node metastases. Two IFP values were recorded in each tumor as shown above, and the lower value did not differ between metastatic and non-metastatic tumors in any of the models ($P > .05$ for HL-16 and Panc-1; Figure 5*A*). The mean of the two IFP values was slightly higher in metastatic than in non-metastatic tumors, with P values of borderline significance of .040 for HL-16 tumors and .055 for Panc-1 tumors (Figure 5*B*). The higher of the two IFP values, on the other hand, was substantially higher in the metastatic than in the non-metastatic tumors in both tumor models ($P = .015$ for HL-16 and $P = .014$ for Panc-1; Figure 5*C*).

Discussion

It has been recognized for several decades that tumors develop elevated IFP during growth [31,32]. Mathematical modeling has suggested that IFP is uniformly elevated in tumors except at the surface where it drops abruptly to normal tissue values [33]. This IFP profile has been demonstrated experimentally in a few rodent and xenografted human tumors [7,17,18]. To avoid breaking the micropipette probe during the IFP measurements, these experiments were carried out with tumors that were soft and had low cell density, high fluid content, and uniform histology with sparse extracellular matrix components. Most likely, the resistance to interstitial fluid flow was low in these tumors as it is in A-07 tumors [7], resulting in a homogeneous IFP level throughout the central tumor region [2,15].

In the work reported herein, intratumor heterogeneity in IFP was studied in tumors with an extensive extracellular matrix by using intramuscular HL-16 cervical carcinoma and Panc-1 pancreatic carcinoma xenografts as tumor models. The intramuscular site is an ectopic site for cervical and pancreatic cancer, and therefore, the microenvironment of intramuscular HL-16 and Panc-1 tumors may not necessarily be similar to the complex microenvironment of human

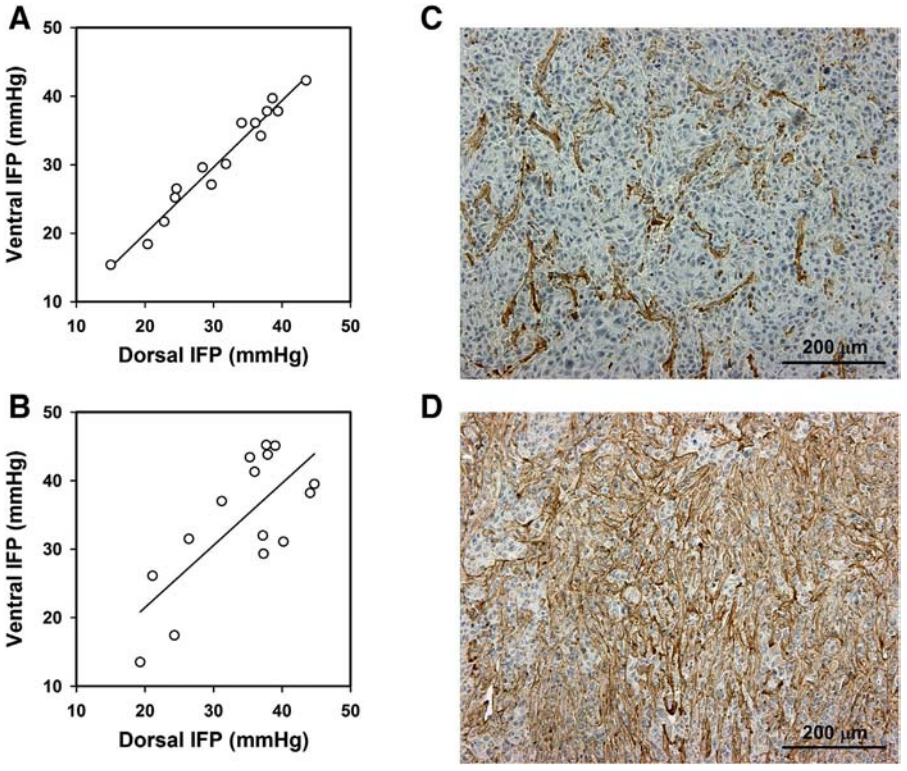

Figure 4. IFP in Panc-1 tumors. IFP measured from the ventral side *versus* IFP measured from the dorsal side for (A) 15 tumors with a sparse extracellular matrix ($P < .0001$; $R^2 = .96$) and (B) 15 tumors with a dense extracellular matrix ($P = .0023$; $R^2 = .54$). The points represent single tumors. (C) Example of a tumor with a sparse extracellular matrix. (D) Example of a tumor with a dense extracellular matrix.

cervical and pancreatic tumors. Orthotopic transplantation was not used in this study because accurate positioning of IFP probes requires surface tumors. Intramuscular transplantation was preferred to subcutaneous transplantation because subcutaneous HL-16 and Panc-1 tumors, in contrast to their intramuscular counterparts, develop large central necroses during growth. Moreover, it should be noticed that the histological appearance of intramuscular HL-16 and Panc-1 tumors is similar to that of cervical and pancreatic tumors in humans [25,30].

IFP is generally higher in intramuscular than in subcutaneous tumors, possibly because the resistance to interstitial fluid flow from the tumor tissue into the surroundings is higher in muscle tissue than in the subcutaneous space [34]. The IFP values measured in our study ranged from 12 to 48 mmHg (HL-16) and from 13 to 45 mmHg (Panc-1). These values are within the same range as those measured in intramuscular tumor models of several cancer types [34], in transgenic mouse models of pancreatic carcinoma [35], and in human cervical carcinoma [10,21].

The current study showed that IFP may differ substantially among different positions within the central region of experimental tumors. Significant intratumor heterogeneity in IFP was associated with the presence of thick connective tissue structures that divided the tumor parenchyma into distinct compartments in HL-16 cervical carcinoma xenografts. In Panc-1 pancreatic carcinoma xenografts, the intratumor heterogeneity in IFP was associated with the presence of a dense collagen-I-rich extracellular matrix. It is highly probable that these tissue stromal elements represented a barrier against interstitial convection, thus preventing local differences in IFP from being leveled out by intratumoral fluid flow.

Intratumor heterogeneity in IFP has been studied in several types of human cancer by measuring IFP in multiple sites within the same lesion, and the variation in IFP was reported to be as great as 2–3-fold in most cancer types [19,20]. In a study of 77 cervical cancer patients, IFP varied by a factor of up to 15 between different measurement sites within single tumors, and the variation in IFP between and within tumors accounted for 41% and 59% of the total sample variance, respectively, implying that the intratumor heterogeneity was larger than the intertumor heterogeneity [21]. In comparison, the ventral and dorsal IFP values of HL-16 and Panc-1 tumors differed by a factor of up to 1.5 only, and there was a significant correlation between the two IFP values in both tumor models, suggesting that tumors showing high IFP in one measurement site generally had developed high IFP and *vice versa*.

In previous studies, we have shown that the development of lymph node metastases is associated with high IFP in the primary tumor in human melanoma, cervical carcinoma, and pancreatic carcinoma xenografts [7,9,30,36,37]. In those studies, tumor IFP was measured in a single position in the tumor center assuming that IFP was uniformly elevated throughout the central tumor region. The current study showed that high IFP is an important determinant of lymph node metastasis also in tumors having developed barriers against intratumoral fluid flow. Interestingly, of the two IFP values measured in each tumor, only the higher value was higher in metastatic than in non-metastatic tumors, suggesting that the metastatic propensity of HL-16 and Panc-1 tumors is determined primarily by the tumor region having the highest IFP. This suggestion is consistent with the proposal that high IFP is associated with high metastatic propensity because hem- and lymphangiogenic factors, proteolytic enzymes, cytokines, and other metastasis-promoting molecules are transported from the primary tumor into peritumoral lymphatics by IFP-driven peritumoral interstitial fluid flow [38,39].

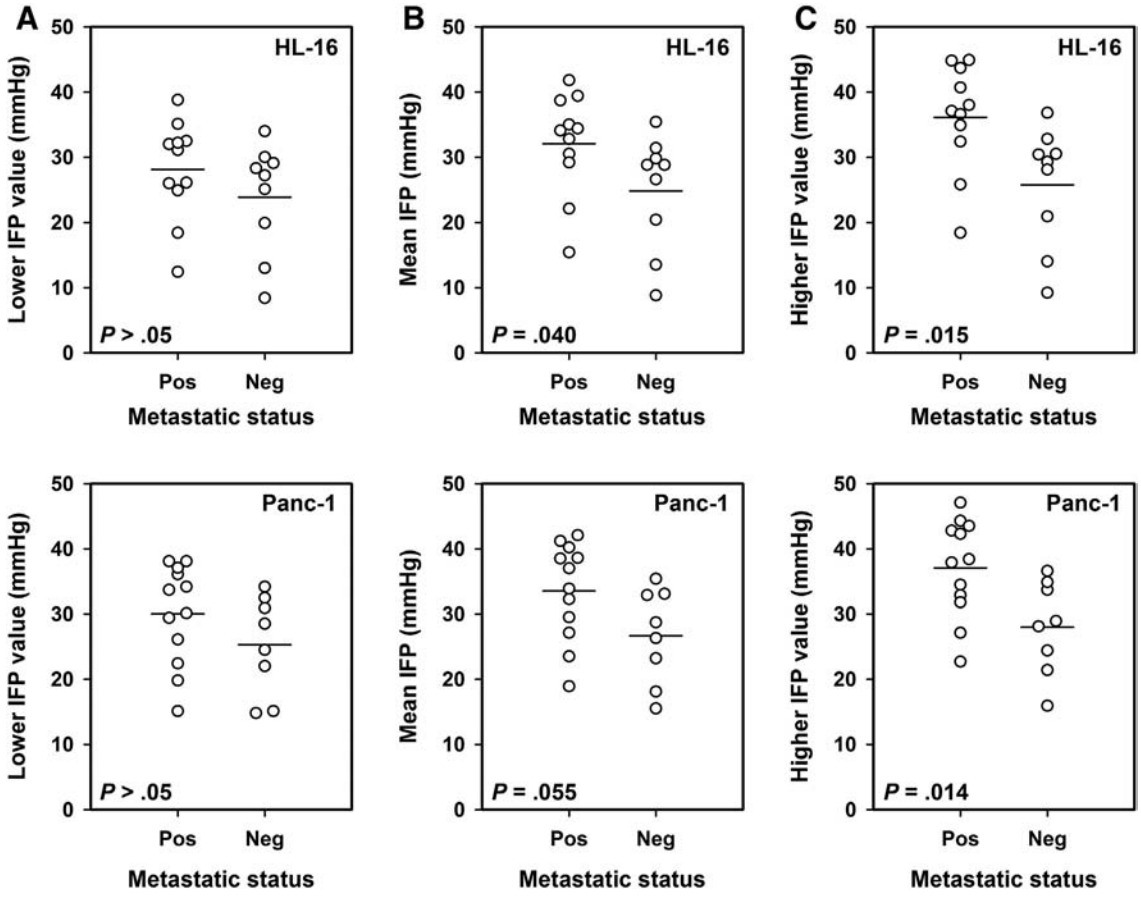

Figure 5. Tumor IFP and host metastatic status. IFP was measured in two positions in HL-16 and Panc-1 tumors, and the plots show (A) the lower, (B) the mean, and (C) the higher of the two IFP values in metastatic and non-metastatic tumors. Twenty mice with HL-16 tumors and 20 mice with Panc-1 tumors were included in the study. The points represent single tumors. The horizontal lines indicate mean values.

Causes and consequences of elevated IFP in tumors have been studied extensively, and most studies have assumed that the resistance to interstitial fluid flow is low in tumor tissue [1,3,15,40]. The current study suggests that this assumption is not necessarily valid for tumors developing a complex, dense, and heterogeneous stroma. On the contrary, our study provides significant evidence that interstitial fluid flow in tumors can be inhibited by fibrotic stromal components, resulting in substantial intratumor heterogeneity in IFP. This is an important observation, which for several reasons should be taken into consideration in future physiological, biological, and therapeutic studies of cancer. First, barriers against interstitial convection may have significant implications for the distribution of all kinds soluble molecules produced and secreted by cancer and stromal cells as well as for the distribution of chemical therapeutic agents. Moreover, as demonstrated in this study, relationships between IFP and tumor metastatic propensity cannot be studied properly without assessing the intratumor heterogeneity in IFP. Similarly, knowledge of the intratumor heterogeneity in IFP may be essential in studies investigating consequences of interstitial hypertension for tumor response to therapy and clinical outcome.

Accurate measurement of interstitial hypertension in human tumors with IFP probes is technically challenging, time consuming, and can only be performed for superficial tumors. Significant efforts are currently being made to develop MRI-based assays for assessment of tumor IFP, and promising assays have been reported [8,41,42]. However, these assays are in an early stage of development, and strategies for improving the assays are currently under investigation. To be of high clinical usefulness, novel MRI-based IFP assays should be capable of providing images mirroring the intratumor heterogeneity in IFP.

In summary, the IFP of HL-16 cervical carcinoma xenografts and Panc-1 pancreatic carcinoma xenografts was measured in two positions in the tumor center, and the IFP values in these measurement sites could differ by a factor of up to 1.5 in both tumor models. This intratumor heterogeneity in IFP was associated with the presence of stromal structures that may have prevented efficient intratumoral interstitial fluid flow. The propensity of the tumors to develop lymph node metastases was associated with the higher but not with the lower of the two IFP values. Intratumor heterogeneity in IFP may have significant implications for tumor aggressiveness and treatment outcome.

References

[1] Heldin CH, Rubin K, Pietras K, and Östman A (2004). High interstitial fluid pressure—an obstacle in cancer therapy. *Nat Rev Cancer* **4**, 806–813.

[2] Lunt SJ, Fyles A, Hill RP, and Milosevic M (2008). Interstitial fluid pressure in tumors: therapeutic barrier and biomarker of angiogenesis. *Future Oncol* **4**, 793–802.

[3] Jain RK (1996). Delivery of molecular medicine to solid tumors. *Science* **271**, 1079–1080.

[4] Cairns R, Papandreou I, and Denko N (2006). Overcoming physiologic barriers to cancer treatment by molecularly targeting the tumor microenvironment. *Mol Cancer Res* **4**, 61–70.

[5] Rofstad EK, Gaustad JV, Brurberg KG, Mathiesen B, Galappathi K, and Simonsen TG (2009). Radiocurability is associated with interstitial fluid pressure in human tumor xenografts. *Neoplasia* **11**, 1243–1251.

[6] Rofstad EK, Ruud EBM, Mathiesen B, and Galappathi K (2010). Associations between radiocurability and interstitial fluid pressure in human tumor xenografts without hypoxic tissue. *Clin Cancer Res* **16**, 936–945.

[7] Rofstad EK, Tunheim SH, Mathiesen B, Graff BA, Halsør EF, Nilsen K, and Galappathi K (2002). Pulmonary and lymph node metastasis is associated with primary tumor interstitial fluid pressure in human melanoma xenografts. *Cancer Res* **62**, 661–664.

[8] Hompland T, Ellingsen C, Øvrebø KM, and Rofstad EK (2012). Interstitial fluid pressure and associated lymph node metastasis revealed in tumors by dynamic contrast-enhanced MRI. *Cancer Res* **72**, 4899–4908.

[9] Rofstad EK, Galappathi K, and Mathiesen BS (2014). Tumor interstitial fluid pressure—A link between tumor hypoxia, microvascular density, and lymph node metastasis. *Neoplasia* **16**, 586–594.

[10] Milosevic M, Fyles A, Hedley D, Pintilie M, Levin W, Manchul L, and Hill R (2001). Interstitial fluid pressure predicts survival in patients with cervix cancer independent of clinical prognostic factors and tumor oxygen measurements. *Cancer Res* **61**, 6400–6405.

[11] Fyles A, Milosevic M, Pintilie M, Syed A, Levin W, Manchul L, and Hill RP (2006). Long-term performance of interstitial fluid pressure and hypoxia as prognostic factors in cervix cancer. *Radiother Oncol* **80**, 132–137.

[12] Yeo SG, Kim JS, Cho MJ, Kim KH, and Kim JS (2009). Interstitial fluid pressure as a prognostic factor in cervical cancer following radiation therapy. *Clin Cancer Res* **15**, 6201–6207.

[13] Hompland T, Lund KV, Ellingsen C, Kristensen GB, and Rofstad EK (2014). Peritumoral interstitial fluid flow velocity predicts survival in cervical cancer. *Radiother Oncol* **113**, 132–138.

[14] Simonsen TG, Lund KV, Hompland T, Kristensen GB, and Rofstad EK (2018). DCE-MRI–derived measures of tumor hypoxia and interstitial fluid pressure predict outcome in cervical carcinoma. *Int J Radiat Oncol Biol Phys* **102**, 1193–1201.

[15] Milosevic M, Fyles A, and Hill RP (1999). The relationship between elevated interstitial fluid pressure and blood flow in tumors: a bioengineering analysis. *Int J Radiat Oncol Biol Phys* **43**, 1111–1123.

[16] Boucher Y and Jain RK (1992). Microvascular pressure is the principal driving force for interstitial hypertension in solid tumors: implications for vascular collapse. *Cancer Res* **52**, 5110–5114.

[17] Boucher Y, Baxter LT, and Jain RK (1990). Interstitial pressure gradients in tissue-isolated and subcutaneous tumors: implications for therapy. *Cancer Res* **50**, 4478–4484.

[18] Eikenes L, Bruland ØS, Brekken C, and de Lange Davies C (2004). Collagenase increases the transcapillary gradient and improves the uptake and distribution of monoclonal antibodies in human osteosarcoma xenografts. *Cancer Res* **64**, 4768–4773.

[19] Boucher Y, Kirkwood JM, Opacic D, Desantis M, and Jain RK (1991). Interstitial hypertension in superficial metastatic melanomas in humans. *Cancer Res* **51**, 6691–6694.

[20] Less JR, Posner MC, Boucher Y, Borochovitz D, Wolmark N, and Jain RK (1992). Interstitial hypertension in human breast and colorectal tumors. *Cancer Res* **52**, 6371–6374.

[21] Milosevic MF, Fyles AW, Wong R, Pintilie M, Kavanagh MC, Levin W, Manchul LA, Keane TJ, and Hill RP (1998). Interstitial fluid pressure in cervical carcinoma: within tumor heterogeneity, and relation to oxygen tension. *Cancer* **82**, 2418–2426.

[22] Stapleton S, Milosevic M, Tannock IF, Allen C, and Jaffray DA (2015). The intra-tumoral relationship between microcirculation, interstitial fluid pressure and liposome accumulation. *J Control Release* **211**, 163–170.

[23] Rofstad EK, Simonsen TG, Huang R, Andersen LMK, Galappathi K, Ellingsen C, Wegner CS, Hauge A, and Gaustad JV (2016). Patient-derived xenograft models of squamous cell carcinoma of the uterine cervix. *Cancer Lett* **373**, 147–155.

[24] Rofstad EK, Huang R, Galappathi K, Andersen LMK, Wegner CS, Hauge A, Gaustad JV, and Simonsen TG (2016). Functional intratumoral lymphatics in patient-derived xenograft models of squamous cell carcinoma of the uterine cervix: implications for lymph node metastasis. *Oncotarget* **7**, 56986–56997.

[25] Wegner CS, Hauge A, Andersen LMK, Huang R, Simonsen TG, Gaustad JV, and Rofstad EK (2018). Increasing aggressiveness of patient-derived xenograft models of cervix carcinoma during serial transplantation. *Oncotarget* **9**, 21036–21051.

[26] Wegner CS, Hauge A, Simonsen TG, Gaustad JV, Andersen LMK, and Rofstad EK (2018). DCE-MRI of sunitinib-induced changes in tumor microvasculature and hypoxia: a study of pancreatic ductal adenocarcinoma xenografts. *Neoplasia* **20**, 734–744.

[27] Rofstad EK and Mathiesen B (2010). Metastasis in melanoma xenografts is associated with tumor microvascular density rather than extent of hypoxia. *Neoplasia* **12**, 889–898.

[28] Rofstad EK, Galappathi K, Mathiesen B, and Ruud EB (2007). Fluctuating and diffusion-limited hypoxia in hypoxia-induced metastasis. *Clin Cancer Res* **13**, 1971–1978.

[29] Hompland T, Ellingsen C, Galappathi K, and Rofstad EK (2014). Connective tissue of cervical carcinoma xenografts: associations with tumor hypoxia and interstitial fluid pressure and its assessment by DCE-MRI and DW-MRI. *Acta Oncol* **53**, 6–15.

[30] Andersen LMK, Wegner CS, Simonsen TG, Huang R, Gaustad JV, Hauge A, Galappathi K, and Rofstad EK (2017). Lymph node metastasis and the physicochemical microenvironment of pancreatic ductal adenocarcinoma xenografts. *Oncotarget* **8**, 48060–48074.

[31] Young JS, Lumsden CE, and Stalker AL (1950). The significance of the tissue pressure of normal testicular and of neoplastic (Brown-Pearce carcinoma) tissue in the rabit. *J Pathol Bacteriol* **62**, 313–333.

[32] Wiig H, Tveit E, Hultborn R, Reed RK, and Weiss L (1982). Interstitial fluid pressure in DMBA-induced rat mammary tumours. *Scand J Clin Lab Invest* **42**, 159–164.

[33] Baxter LT and Jain RK (1989). Transport of fluid and macromolecules in tumors. 1. Role of interstitial pressure and convection. *Microvasc Res* **37**, 77–104.

[34] Lunt SJ, Kalliomäki TMK, Brown A, Yang VX, Milosevic M, and Hill RP (2008). Interstitial fluid pressure, vascularity and metastasis in ectopic, orthotopic and spontaneous tumours. *BMC Cancer* **8**(2).

[35] Chauhan VP, Boucher Y, Ferrone CR, Roberge S, Martin JD, Stylianopoulos T, Bardeesy N, DePinho RA, Padera TP, and Munn LL, et al (2014). Compression of pancreatic tumor blood vessels by hyaluronan is caused by solid stress and not interstitial fluid pressure. *Cancer Cell* **26**, 14–15.

[36] Hompland T, Ellingsen C, Galappathi K, and Rofstad EK (2014). DW-MRI in assessment of the hypoxic fraction, interstitial fluid pressure, and metastatic propensity of melanoma xenografts. *BMC Cancer* **14**, 92.

[37] Ellingsen C, Walenta S, Hompland T, Mueller-Klieser W, and Rofstad EK (2013). The microenvironment of cervical carcinoma xenografts: associations with lymph node metastasis and its assessment by DCE-MRI. *Trans Oncol* **6**, 607–617.

[38] Mumprecht V and Detmar M (2009). Lymphangiogenesis and cancer metastasis. *J Cell Mol Med* **13**, 1405–1416.

[39] Shields JD, Fleury ME, Yong C, Tomei AA, Randolph GJ, and Swartz MA (2007). Autologous chemotaxis as a mechanism of tumor cell homing to lymphatics via interstitial flow and autocrine CCR7 signaling. *Cancer Cell* **11**, 526–538.

[40] Ariffin AB, Forde PF, Jahangeer S, Soden DM, and Hinchion J (2014). Releasing pressure in tumors: what do we know so far and where do we go from here? A review. *Cancer Res* **74**, 2655–2662.

[41] Walker-Samuel S, Roberts TA, Ramasawmy R, Burrell JS, Johnson SP, Siow BM, Richardson S, Goncalves MR, Pendse D, and Robinson SP, et al (2018). Investigating low-velocity fluid flow in tumors with convection-MRI. *Cancer Res* **78**, 1859–1872.

[42] Elmghirbi R, Nagaraja TN, Brown SL, Keenan KA, Panda S, Cabral G, Bagher-Ebadian H, Divine GW, Lee IY, and Ewing JR (2018). Toward a noninvasive estimate of interstitial fluid pressure by dynamic contrast-enhanced MRI in a rat model of cerebral tumor. *Magn Reson Med* **80**, 2040–2052.